

GT2011-46573

HEAT TRANSFER FOR THE FILM-COOLED VANE OF A 1-1/2 STAGE HIGH-PRESSURE TRANSONIC TURBINE – PART II: EFFECT OF COOLING VARIATION ON THE VANE AIRFOIL AND INNER ENDWALL

Harika S. Kahveci, Charles W. Haldeman, Randall M. Mathison, and Michael G. Dunn
 The Ohio State University Gas Turbine Laboratory
 Columbus, OH 43235

ABSTRACT

The impact of film cooling on heat transfer is investigated for the high-pressure vane of a one-and-one-half stage high-pressure turbine operating at design corrected conditions. Cooling is supplied through three independently controllable circuits to holes in the inner and outer endwall, vane leading edge showerhead, and the pressure and suction surfaces of the airfoil in addition to vane trailing edge slots. Four different overall cooling flow rates are investigated and one cooling circuit is varied independently. All results reported in this part of the paper are for a radial inlet temperature profile, one of the four profiles reported in Part I of this paper. Part I describes the experimental setup, data quality, influence of inlet temperature profile, and influence of cooling when compared to a solid vane.

This part of the paper shows that the addition of coolant reduces airfoil Stanton Number by up to 60%. The largest reductions due to cooling are observed close to the inner endwall because the coolant to the majority of the vane is supplied by a plenum at the inside diameter. While the introduction of cooling has a significant impact on Stanton Number, the impact of changing coolant flow rates is only observed for gauges near 5% span and on the inner endwall. This indicates that very little of the increased coolant mass flow reaches all the way to 90% span and the majority of the additional mass flow is injected into the core flow near the plenum.

Turning off the vane outer cooling circuit that supplies coolant to the outer endwall holes, vane trailing edge slots, and three rows of holes on the pressure surface of the airfoil, has a local impact on Stanton Number. Changes downstream of the holes on the airfoil pressure surface indicate that internal heat transfer from the coolant flowing inside the vane is important to the external heat transfer, suggesting that a conjugate heat-transfer solution may be required to achieve good external heat-transfer predictions in this area. Measurements on the inner endwall show that temperature reduction in the vane wake due

to the trailing edge cooling is important to many points downstream of the vane.

NOMENCLATURE

A	Area
BR	Blowing Ratio
	$\frac{\rho V _{Cooling}}{\rho V _{Core}}$
c	Coolant (subscript)
C_p	Constant Pressure Specific Heat
d	Cooling Hole Diameter
f	With Film Cooling (subscript)
NSR	Net Stanton Reduction,
	$NSR = \frac{St_o - St_f}{ St_o }$
q''	Heat Flux
ref	Reference (subscript)
St	Stanton Number (global),
	$St = \frac{q''}{A_{ref} [\dot{m} (C_p T)_{ref} - (C_p T)_w]}$
T	Local Temperature
T_{avg}	Average Temperature
$T_{0,inlet}$	Turbine Inlet Bulk Temperature
w	At a Wall Boundary (subscript)
x	Distance on Wetted Surface
\dot{m}	Turbine Mass Flow Rate
0	Without Film Cooling (subscript)

1. INTRODUCTION

This part of the paper is intended to build on the results presented in Part I and further explore the impact of varying the coolant flow rates. As discussed in Part I, this study is intended to provide a macroscopic view of the impact of cooling on vane heat transfer while providing information to aid in the understanding of more localized effects. This perspective and

the corresponding selection of Stanton Number definition and analysis techniques provides results in a form that are easily scaled to an engine application.

In order to provide better context for this discussion, the literature review in this part of the paper presents the development of analysis techniques using these two perspectives. There are a tremendous number of publications dealing with the local effects of blowing ratio, momentum ratio, hole shape, and other factors for simplified geometries, which we will refer to as microscopic studies. Macroscopic studies are slightly less common since they typically require more complicated experimental setups that capture more of the realistic engine geometry. However, there are sufficient numbers of publications in both categories that only representative summaries can be provided here.

Many of the earliest microscopic level studies reported the impact of hole geometry and coolant density on film cooling and were summarized by Goldstein et al. [1]. Since then, there have been numerous experimental publications using flat-plate configurations and concentrating on the geometry of holes (such as shape and orientation), the interaction of rows of holes, or the impact of flow parameters. Other studies have addressed these same questions using more complicated cascade geometries [2-4]. Bogard and Thole provide a good summary of these types of studies in [5]. Recent studies performed at EPF Lausanne have carefully investigated the impact of varying coolant injection parameters on film effectiveness for leading edge and inner endwall flow and have also achieved impressive agreement with numerical predictions [6-8].

Investigations from a wider perspective are most common for the inner endwall, where cooling distribution is often dominated by vortex structure rather than the physics of local mixing. Pioneering work performed by Blair [9] described turbine endwall heat transfer with coolant injection upstream of the vane leading edge in a cascade. Heat transfer levels were found to be greater near the leading edge due to the local vortex structure. Many subsequent studies such as that of Langston [10] have worked to better define the vane endwall flow pattern even in the absence of cooling. Simon and Piggush provide a good overview of research into endwall vortex structure [11]. The accumulated work of Friedrichs et al. contributed a very interesting perspective on the interaction of cooling with the endwall vortex structure and how this resulted in larger changes of cooling distribution [12-14]. Kost and Nicklas adopted a wide perspective on the same question but also investigated the impact of overall blowing ratio for a cascade [4, 15].

A macroscopic viewpoint has also been applied when studying the impact of hot streak temperature profiles on vane heat transfer. Jenkins et al. investigated the impact of film cooling on hot streak dissipation [16], while Varadarajan et al. investigated the impact of the hot streak on the vane heat transfer [17]. These studies found that hot streaks caused strong surface temperature gradients, but that proper definition of parameters collapsed the adiabatic film effectiveness to nearly the same values. Barringer et al. reached similar conclusions using an annular cascade [18, 19].

The studies summarized here indicate that there are significant precedents for addressing cooling issues from multiple perspectives. The more general viewpoint adopted for much of this paper will describe the overall distribution of cooling and highlight regions where more study is necessary, while providing some insight into local behavior.

2. EXPERIMENT DESCRIPTION

This experiment is described in detail in Part I [20] of this paper and in the earlier papers of Mathison et al. [21-25]. The experimental vehicle is a turbine operating at design-corrected conditions with a fully cooled high-pressure vane, a high-pressure rotor with solid blades, and a solid low-pressure vane. Additional coolant is added through the purge cavity between the high-pressure vane and the rotor. A passive heat exchanger capable of creating uniform, radial, and hot-streak profiles is installed at the inlet to the turbine stage.

2.1 Instrumentation

While there is a wide variety of instrumentation installed in the stage, this paper will focus on the double-sided Kapton heat-flux gauges installed on the cooled high-pressure vane. These gauges are installed in four constant span arrays on multiple vane airfoils to provide a map of the heat-flux. Gauges are located at 5%, 15%, 50%, and 90% span and at wetted distances from -75% on the pressure surface to 95% on the suction surface (see part I). Additional gauges are installed on the inner endwall, as illustrated in Figure 1. Crosses are used to illustrate locations where only a single side of the gauge is available to provide temperature measurements, and crosses with boxes indicate gauges that have a surviving pair so that both temperature and heat flux measurements are available.

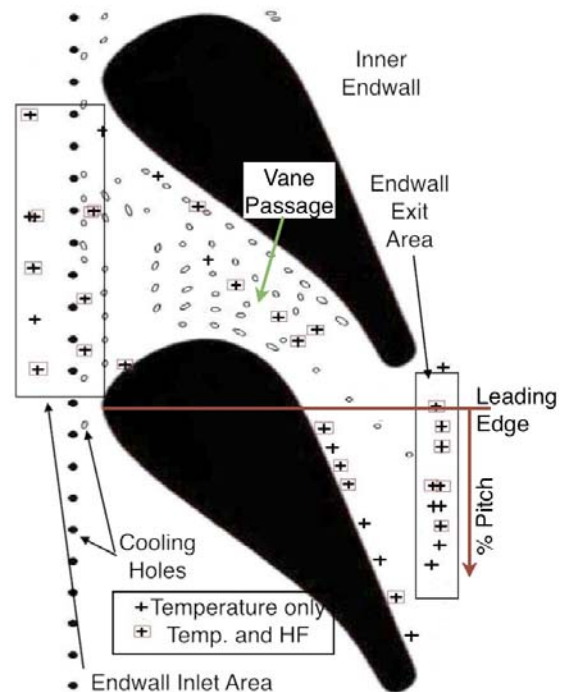


Figure 1. Location of inner endwall heat-flux gauges

All gauges on the inner endwall and on the vane airfoil are carefully placed to avoid blocking cooling holes. The electrical leads are painted in place with a conductive paint to avoid covering the holes or disrupting airflow.

2.2 Run Conditions

Part I of this paper outlines seventeen run conditions available for analyzing vane heat transfer that are chosen to provide insight into the effect of inlet temperature profile and cooling levels. The influence of inlet temperature profile on vane surface heat transfer is discussed in Part I, and this part will focus on a subset of runs chosen to determine the effect of coolant level variation for a radial inlet temperature profile. Table 1 provides a summary of the differences among these repeat conditions.

Cooling Flow Rate	Vane Inner (%)	Vane Outer (%)	Purge (%)
None	0	0	0
Low	4.58±0.11	4.29±0.10	1.64±0.04
Nominal	6.93±0.03	5.40±0.02	0.70±0.00
High	8.06±0.00	6.28±0.00	0.82±0.00
No Vane Outer	7.08±0.04	0	0.72±0.00

Table 1. Summary of cooling conditions

Part I also demonstrated the overall influence of cooling by presenting comparisons of the Stanton Number measurements for two separate experimental builds: an older experiment with solid vane airfoils and the current experiment with a cooled vane. In contrast, this part of the paper only draws data from the cooled geometry used in the most recent experiment. The no cooling case here represents the measurements acquired for the cooled geometry, but with all of the coolant flow turned off.

Three independent cooling circuits supply the vane inner circuit, the vane outer circuit, and the purge cavity downstream of the vane. The vane inner circuit supplies cooling gas to the leading edge, the majority of the airfoil surface, and the inner endwall. The trailing edge, last three rows of holes on the pressure surface, and outer endwall are supplied via the vane outer circuit. Table 2 gives the split of the cooling rows and the area ratios of total number of holes per circuit. As reference, the average total-to-total pressure ratio is 4.58 and the average corrected speed is 370.5 rpm/K^{1/2}. The cooling scheme is typical of a modern impingement/film-cooled system with cylindrical holes of various sizes and angles.

Circuit	Location	% of Circuit Area	No. of Rows
Vane Inner	Vane Airfoil (PS & SS)	79.6	13
	Inner Endwall	20.4	-
Vane Outer	Vane Airfoil	20.2	3
	TE Slots (PS)	23.5	-
	Outer Endwall	56.3	-

Table 2. Vane cooling circuit area distribution

The inlet temperature profile is fairly consistent from run to run, but there are small changes that cause visible differences in the measured heat transfer. Figure 2 presents the average inlet temperature profiles measured for each cooling level. For this and all subsequent plots, the range bars represent the variation observed among the repeat runs for each condition.

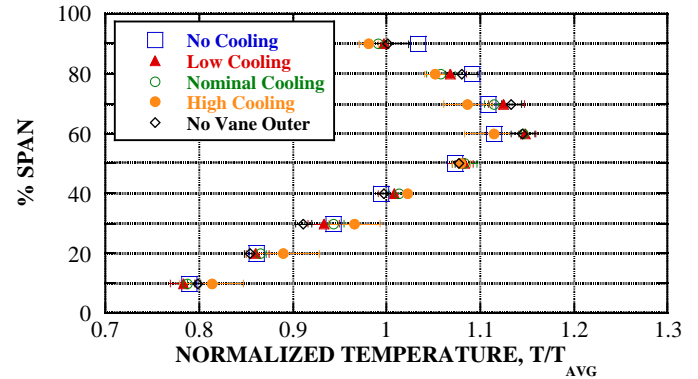


Figure 2. Inlet temperature profile shapes for cooling comparison runs

These small changes in profile shape may cause corresponding differences in the heat-flux measurements, but the Stanton Number (global) definition presented in Equation 1 is designed to account for these changes:

$$St = \frac{q''}{\frac{\dot{m}}{A_{ref}} [(C_p T)_{ref} - (C_p T)_w]} \quad (1)$$

T_{ref} is chosen to be the inlet temperature measured at the same span as the heat-flux gauge of interest, i.e. a gauge at 90% span utilizes the inlet temperature measured at 90% span. Part I discussed the benefits of an alternate Stanton Number definition but also demonstrated that the formulation described here provides a good representation of the measured heat flux that is easily generalized and accounts for some variations in the experimental boundary conditions. This definition is not sufficient to completely account for all differences in profile shape, but it is effective in accounting for small changes from one run to the next.

Much of the data presented here will be expressed in Stanton Number, but comparisons among multiple cooling conditions may also be expressed using the Net Stanton Number Reduction, defined in Equation 2.

$$NSR = \frac{St_0 - St_f}{|St_0|} \quad (2)$$

This parameter is based on the Net Heat Flux Reduction (NHFR) parameter originally proposed by Sen et al. [26]. It compares the Stanton Number for a case of interest (St_f) to a baseline case (St_0). This is different from a local measure of adiabatic film effectiveness since the Stanton numbers are defined based on global properties and not the adiabatic wall temperature. The advantage of this system for the work presented here is that changes between bulk conditions are accounted for with directly measured properties and can be related back to the stage control inputs (inlet temperature profile and level, and cooling levels). In contrast, a local film effectiveness assumes that the adiabatic wall temperature is the main driving factor and that it is only changed by well-known alterations to the main boundary conditions. The adiabatic film effectiveness is therefore optimized for a different type of analysis than the one undertaken herein, and the NSR provides a more direct method of tracking the impact of cooling for this experiment.

3. EFFECT OF OVERALL COOLING VARIATION

This section explores the influence of varying the overall coolant flow rate. Comparisons are made between the no cooling case, and the low, nominal, and high coolant flow rates. It will be shown that while all three of the cooling cases provide a significant reduction in Stanton Number from the uncooled condition, the additional coolant flow of the higher flow rate cases is primarily injected into the core flow nearer to the hub and therefore only has a small impact on the full airfoil surface.

Figure 3 presents the spanwise averaged Stanton Numbers for the four different cooling cases of interest. Gauges at the same wetted distances but different spans are averaged together to provide an indication of the combined difference between cases.

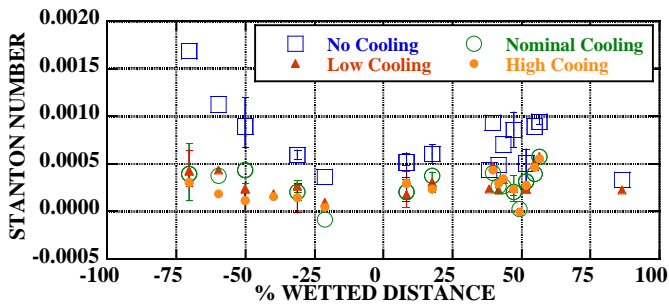


Figure 3. Spanwise averaged Stanton Number distribution

The effect of introducing cooling is quite clear; the no cooling case (blue) has substantially higher Stanton Numbers than all of the cases including cooling. This may seem like an obvious conclusion based on the cooling comparison presented in Part I that looked at the Stanton Number observed for nominal cooling and for a solid vane version of this experiment. However, one must remember that a key finding of

that comparison was that measurements for the vane with cooling holes but no coolant flow are quite different than for a solid vane due to ingestion through the cooling holes on the pressure surface and re-injection of that flow through the vane suction surface. Figure 3 shows that even though there is still some ingestion in the no cooling case, the introduction of the low-temperature cooling flow has a much more pronounced impact on the Stanton Number at all wetted distances.

In order to better identify the differences among the low, nominal, and high cooling cases, it is helpful to plot this information using the Net Stanton Number Reduction (NSR) parameter. Figure 4 presents the Net Stanton Number Reduction for each span evaluated using the no cooling case as a baseline. This means that an NSR value of 0.6 represents a 60% reduction in Stanton Number from the no cooling case.

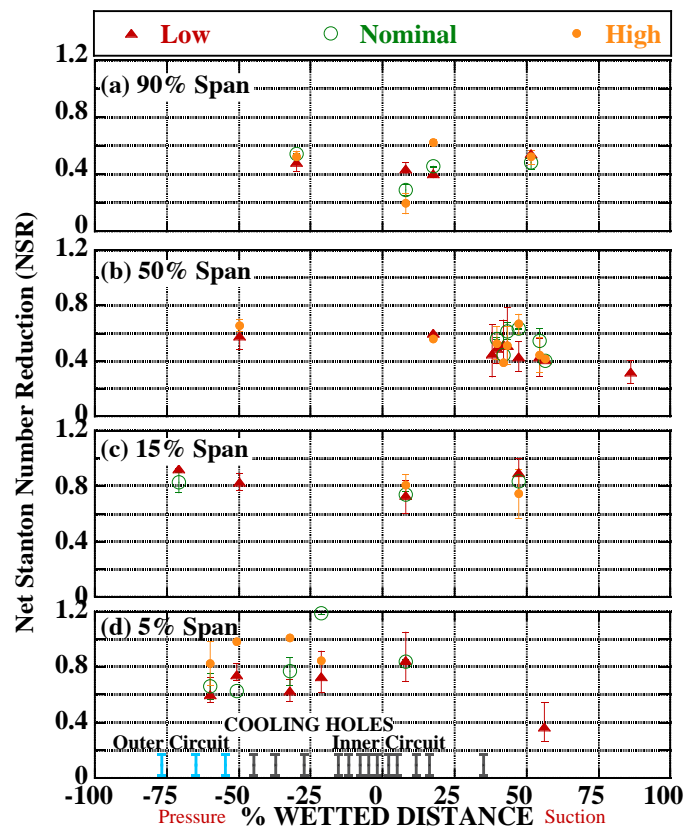


Figure 4. Net Stanton reduction due to cooling variation for airfoil surface

Looking at each span independently, it is possible to pick out a few points where the variation in cooling flow rate caused notable differences in Stanton Number. The majority of these points show a slightly larger reduction for the high cooling case and a smaller reduction for the low cooling case. However, there are a few points that show a contrary trend, and the majority of points do not show any discernible difference due to cooling. Only at 5% span can one observe a consistently higher reduction in Stanton Number due to the higher cooling flow rates.

At the same time, if one compares the general level of Stanton Number reduction for 5%, 15%, 50%, and 90% span, the cooling clearly has a greater effect at the spans closer to the hub. The majority of the cooling rows (all of those indicated by gray symbols) are supplied by the vane inner circuit, which feeds from a circumferential plenum located at the hub of the vane airfoil. Coolant must therefore traverse most of the span of the airfoil before it is ejected at 90% span. Typical coolant temperatures are between 295 and 325K based on location and the experiment, and these temperatures are generally 10-30 degrees below the metal temperature. This means that as the coolant flows through the inside of the vane to the outer spans, it picks up heat from the vane surface causing a reduction in mass flow and an increase in coolant temperature. This is reflected by the smaller influence of cooling on the outer spans. This also demonstrates why the global definitions of Stanton number can help isolate areas of cooling effectiveness (or lack thereof) even without exact knowledge of the local conditions. This information, combined with the observation that increasing the cooling flow rate only causes significant changes in Stanton Number for the gauges at 5% span, suggests that increasing the coolant flow rate to the vane tends to force more coolant out through the holes near to the endwall without causing a substantial change in flow rate to holes at higher spans.

3.1 Overall Cooling Variation for the Endwall

Measurements for the vane inner endwall support this understanding and behave similarly to the measurements presented for 5% span on the airfoil. Figure 5 shows contour plots of the Stanton Number observed for the inner endwall without coolant and with a nominal cooling flow rate. These plots are created by mapping measurement locations from multiple passages to a single passage. The measurement locations are indicated by crosses.

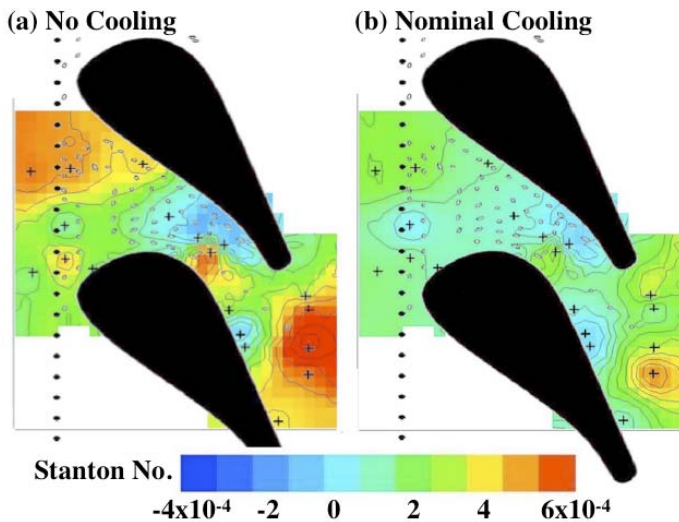


Figure 5. Stanton Number distribution for inner endwall for (a) no cooling and (b) nominal cooling case (geometry not to scale)

The no cooling case shows a very high Stanton Number in the inlet region and downstream of the vane, where the mixing of the vane wake brings high temperature fluid near to the surface and increases the heat transfer. In addition, a region of increased heat transfer appears on the suction side of the vane throat where flow acceleration thins the boundary layer.

Introducing cooling smoothes out this variation across the endwall surface. The line of large cooling holes upstream of the leading edge reduces the Stanton Number across much of the inlet. Small increases in Stanton Number are observed for regions near the pressure surface of the throat due to increased mixing, but the regions of high Stanton Number present without cooling are eliminated. The most notable change due to cooling is that the region of high heat transfer in the vane wake is nearly eliminated by the cooling. Even though the mixing is still present or is even increased with the introduction of cooling, the vane trailing edge coolant reduces the temperature in the vane wake substantially so that only a single gauge detects an increase in Stanton Number due to the wake. The influence of the vane trailing edge cooling will be discussed in more detail in the following section.

One remaining point of interest is the gauge located near mid-pitch just upstream of the first line of cooling holes (located in the orange region for the no cooling case). This gauge shows a significant reduction of Stanton Number due to cooling, but it is upstream of all coolant injection. One possible explanation for this effect is that blockage from the downstream cooling holes slows the flow and allows an increase in boundary layer thickness at this gauge location, causing a reduction in heat transfer coefficient. The converse of this blockage effect is that ingestion is likely occurring for the no cooling case, so it is possible that suction from the large line of holes just downstream of this gauge location draws higher temperature flow closer to the surface. The double-sided Kapton heat-flux gauges and Stanton Number definition should account for any backside heating effects present at this location, but it is also possible that there is an additional physical parameter at work that is not fully captured by the Stanton Number definition.

Because the differences among the cooling flow rates are significantly smaller than those observed between the nominal and un-cooled cases, it is helpful to instead make comparisons among these conditions using contour plots of the Net Stanton Number Reduction. Figure 7 presents the Stanton Number Reduction for the low and high cooling cases relative to the nominal cooling case. Thus, a relative NSR value of 0.2 represents a 20% reduction in Stanton Number from the nominal cooling case while a value of -0.2 represents a 20% increase from the nominal case. It is also important to note that since the Stanton Number for the nominal cooling case is quite close to zero in some locations (as indicated in Figure 5), small changes in Stanton Number will result in large percentage changes. A 200% increase in Stanton Number is therefore not quite as dramatic as it sounds. However, this plot is still quite helpful for identifying the relative influence of the cooling.

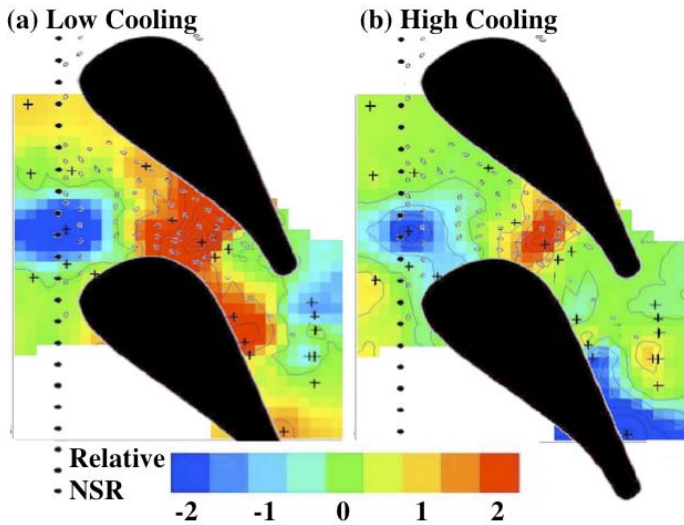


Figure 6. Net Stanton Reduction for nominal cooling versus the (a) low cooling and (b) high cooling cases (geometry not to scale)

One of the most surprising features of this comparison is that the low cooling condition shows a notable reduction in Stanton Number from the nominal case over much of the endwall. This clearly indicates that there is a more complicated interaction causing the cooling benefits than a simple mixing model based on the reduction of temperature caused by a cooler stream of gas. Even though there is less coolant, the lower momentum flow provides significantly better coverage across the passage and stretching aft along the suction surface. The higher flow rate of the nominal case may cause the film cooling jets to penetrate too deeply into the flow where they are swept away by the passage vortex. Moving to the comparison presented in Part (b) of Figure 6, the high cooling case also shows a reduction in Stanton Number in the vane passage. The jets are still likely detaching, but enough more cooling is added to reduce the heat transfer through temperature reduction.

These comparisons highlight the complexity of the endwall flow for a film-cooled vane. It is tempting to try to relate the lift-off effects to local cooling parameters such as the blowing ratio for each hole, since these behaviors have been previously studied in great detail. Computational models indicate that the approximate blowing ratios for the holes distributed across the passage vary from 1.8 to 4.5 for the nominal cooling case. In the throat region where there is particular interest in detachment, the blowing ratios are approximately 1.8-2.1 for the low cooling case, 2.3-2.9 for the nominal cooling case, and 2.4-3.0 for the high cooling case. It may be argued that the increase in blowing ratio causes the detachment of the cooling in this region, and it certainly must play a role. However, one must also consider the complicated interactions of the coolant with the macroscopic structure of the flow. Friedrichs et al. showed that coolant injection upstream of the passage vortex can change the lift off point of vortices and influence downstream coolant distribution [12]. The transonic nature of this turbine further complicates matters since there are a variety

of unsteady shockwave interactions that may be modified in some way by the introduction or change of cooling flows.

The current study is not designed to distinguish among these different effects. Given the difficulty of acquiring measurements in this region with the full complexity of an operating turbine stage, many of the next advances in understanding may come from comparing computational models to the data presented here to improve modeling techniques and gain insight into the flow structure responsible for these changes. However, because the data is displayed normalized by the upstream properties, the changes in heat-flux for the different cases can be observed even without detailed knowledge of the local conditions.

The only parts of the endwall where the low cooling case does not have a reduced or equivalent Stanton Number with respect to nominal cooling (i.e. blue spots) occur immediately downstream of the vane trailing edge and just upstream of the vane leading edge. The increase downstream of the trailing edge indicates in part that the higher coolant flow rate of the nominal case is helpful in reducing the temperature in the vane wake and therefore keeping the Stanton Number lower in this region. Upstream of the leading edge, the region of increased Stanton Number (negative NSR) can be traced to a single gauge. It must be remembered that the Stanton Number indicated for this gauge in Figure 5 is very near to zero, so even though there is a large NSR, there are only small changes in the measurement. This gauge was checked carefully across all experimental runs for problems, but none were found. The gauge shows a lower Stanton Number for the nominal case than both the low and high cooling cases. This may be caused by its close proximity to the large cooling hole just upstream; certain blowing conditions may cause the coolant to impinge directly on the gauge while other conditions may cause the coolant to miss the gauge entirely. Additional measurements are needed in this region to better understand the possible cause of this variation.

3.2 Overall Cooling Variation for Midspan

Another region of interest in the Stanton Number distribution presented in Figure 4 is the cluster of gauges on the suction surface at midspan. These gauges fall immediately behind the last cooling row and represent the region of highest instrument density on the airfoil. It is difficult to observe differences in Stanton Number in this figure, so the data from these gauges is re-plotted as a function of x/D moving aft across the suction surface from the last cooling row. Figure 7 plots both the Net Stanton Number Reduction (relative to the no cooling baseline) and a Relative Stanton Number Reduction (relative to the nominal cooling case) for these gauges.

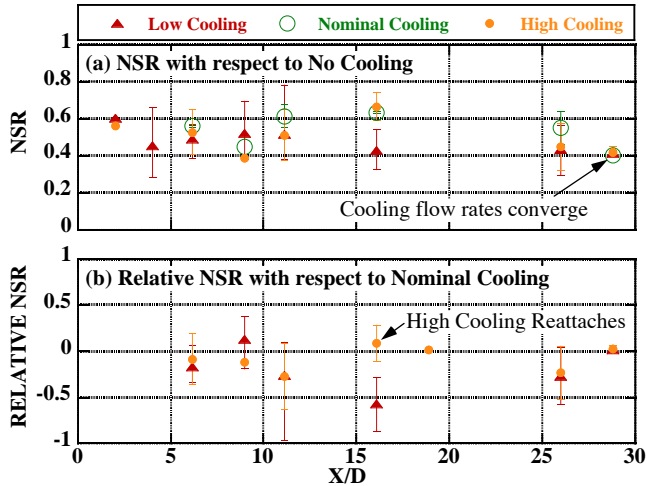


Figure 7. Stanton Number Reduction for suction surface plotted by X/D relative to (a) no cooling (b) nominal cooling

Part (a) of Figure 7 shows once again that while the differences among the cooling flow rates are small, the Stanton Number for any of the cooling cases is reduced 40-70% from the no cooling case. As discussed earlier, one would expect the differences among the cooling cases to be small in Part (b), since much of the added coolant for the higher cooling flow rate cases is injected at the inner endwall and lower spans of the airfoil, and is not expected to influence the midspan gauges plotted here. Part (b) illustrates that general trends can be picked out by cooling level, with the low cooling tending to have a negative Stanton Number Reduction (indicating an increase in heat transfer) and the high cooling case tending to show a small improvement. However, these changes are small compared to the repeatability bars indicated for most points, and other more complicated local effects seem to be at work. The low cooling case shows a small reduction in Stanton Number immediately upstream of $x/D = 10$, and an increase further downstream of this location. This suggests that the jet structure is such that the cooling jet reattaches to the surface near this point but is mixed out moving further downstream. Similarly, the high cooling case shows a negative Relative NSR for the first several gauge locations and does not show any benefit over the nominal case until about $x/D = 15$. This likely indicates that the cooling jet separates from the surface immediately downstream of the hole but reattaches before mixing out. The real mystery gauge in this series is at $x/D = 26$, where the nominal cooling case has a lower Stanton Number than the other cases. One would expect mixing to dominate at

this point on the surface and all three cases to converge towards a common value.

4. EFFECT OF VANE OUTER COOLING

In order to better understand the role of each cooling circuit in controlling vane airfoil and endwall heat transfer, coolant flow rates are varied for individual circuits. The impact of the purge cooling circuit on the vane endwall and airfoil heat-flux measurements is very small [27] and will not be discussed here. Instead, this section will focus on the impact of turning off the vane outer cooling circuit in order to separate the effects of the inner and outer cooling circuits. As described earlier in Table 2, the vane outer circuit supplies the outer endwall, the trailing edge slots (covering the full span of the airfoil), and three rows of holes on the pressure surface. The vane inner circuit supplies the rest of the airfoil film-cooling holes as well as the inner endwall.

Figure 8 presents the heat flux and Stanton Number for gauges installed on the vane airfoil. In this plot, the case labeled "With Vane Outer" is the nominal cooling case described in Table 1. The "No Vane Outer" case has a nearly identical flow rate for the vane inner and purge cooling circuits, but all flow is turned off for the vane outer circuit.

As one might expect, the primary difference between the two cooling cases can be observed for -50 to -80% wetted distance on the pressure surface downstream of the cooling holes supplied by the vane outer circuit. It is surprising to note that the largest difference in Stanton Number occurs at 5% span. At first glance, this seems contrary to the trend observed for the vane inner circuit for the overall cooling variations, which was that higher cooling levels and larger Stanton Number reductions are at the locations closer to the coolant supply plenum. However, the heat flux comparisons for these gauges show that the reduction in heat flux due to the vane outer circuit is fairly consistent for all spans. Referring back to the Stanton Number definition presented in Equation 1, it is clear that since the mass flow and area values used are the same for all gauges and the heat-flux magnitudes are similar, the larger change in Stanton Number at 5% span must be due to a change in driving temperature that is not directly related to heat flux. Changes in external driving temperature cause a change in heat flux that is accounted for in Stanton Number, but it does not account for changes in the backside heat transfer due to conduction from the inside of the cooled cavity. Therefore, the 5% span shows the largest change in Stanton Number since it is most susceptible to ingestion when the coolant is turned off.

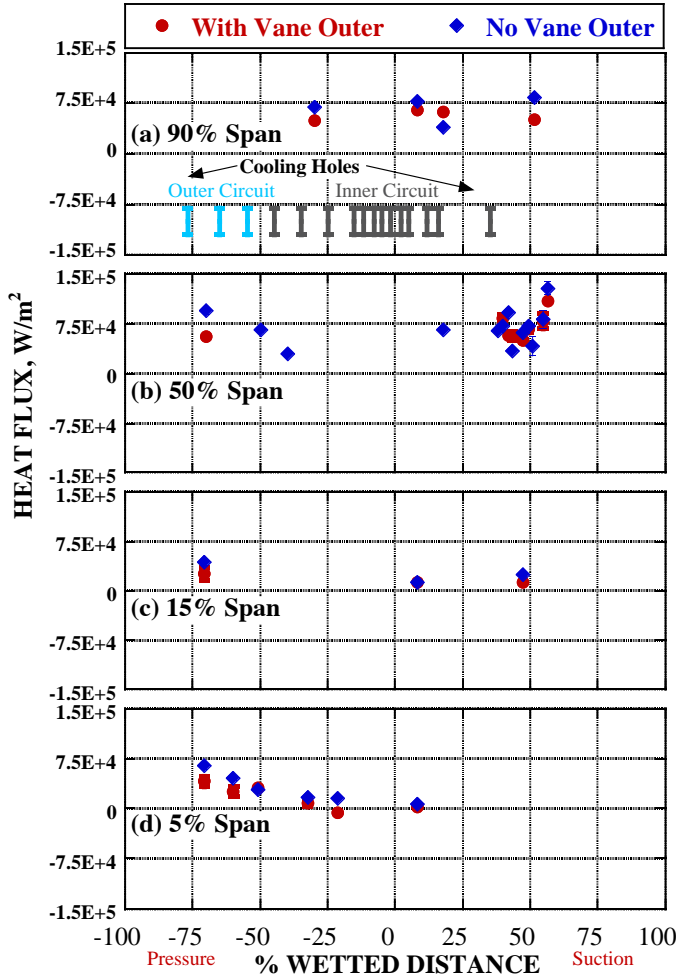


Figure 8. Comparison of (a) heat flux and (b) Stanton Number for vane outer coolant modulation

The impact of the vane outer circuit is also clear for the gauges installed at the inner endwall across the exit of the passage. The Stanton Number for these gauges is presented in Figure 9 by percent pitch moving across the passage.

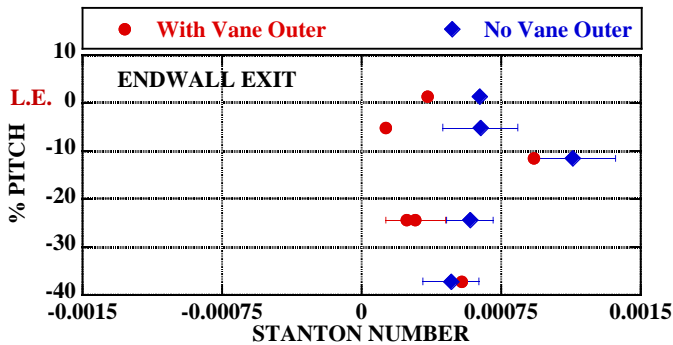
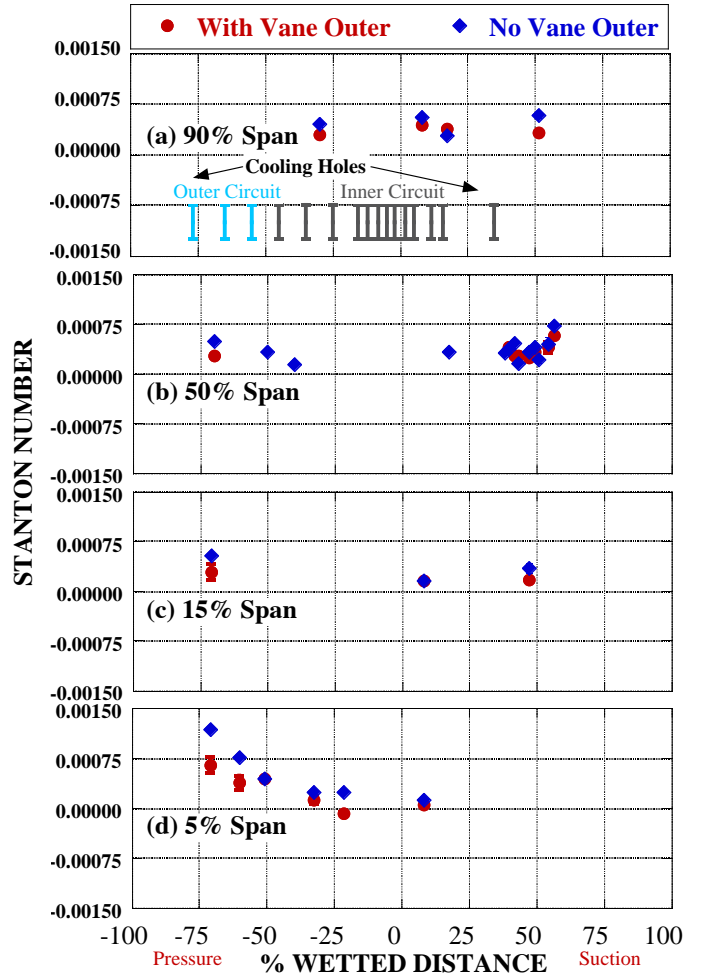


Figure 9. Influence of vane trailing edge cooling on inner endwall Stanton Number

The case with no cooling flow to the vane outer circuit has consistently higher Stanton Numbers than the case with nominal cooling to the vane outer circuit. Only the gauges at -12% pitch and -37% pitch do not demonstrate a significant



difference due to vane outer cooling. It was hypothesized in Section 3 that the vane wake played a significant role in driving the endwall heat transfer in this region, which is confirmed by this plot. Regions of high mixing still eliminate cooling effects at some gauge locations, but other locations experience a reduced Stanton Number because of the temperature reduction in the vane wake due to the trailing edge cooling.

5. SUMMARY

The impact of film cooling on the heat transfer measurements for a high-pressure vane is investigated in detail for a turbine operating at design-corrected conditions with a radial inlet temperature profile. Measurements are compared for cases with all of the cooling flow turned off and with the overall cooling flow set to low, nominal, and high cooling flow rates. In addition, comparisons are presented between the nominal cooling case and a case with nominal cooling for the vane inner and purge circuits while the vane outer circuit is turned off. This makes it possible to isolate the impact of each vane cooling circuit.

The overall cooling variation runs showed that while there is a large difference between the no cooling case and the cooled

runs, the differences among the cooling flow rates are small. Cooling is shown to have a greater effect at the inner endwall and the inner spans since the coolant for nearly the entire airfoil is supplied from a plenum at the inner diameter of the vane ring. Less coolant reaches the outer spans and therefore the cooling has a smaller effect. Increasing the coolant flow rate has a notable impact on the heat transfer measurements for the endwall and inner spans, but does not change the Stanton Number significantly elsewhere on the airfoil. This indicates that increasing the coolant flow rate has the effect of increasing the coolant from holes closer to the plenum, but very little of this additional mass flow is transmitted to the 50% or 90% span locations.

The inner endwall has a very complicated Stanton Number distribution. Coolant blends out variation across the passage and reduces the Stanton Number significantly at most locations. Surprisingly, the lowest Stanton Numbers are obtained for the low coolant flow rate. Increasing the coolant flow rate to the nominal or high cooling conditions tends to increase the Stanton Number at most locations due to increased mixing, blow-off of the protective film, or changes in the external flow structure.

Varying the vane outer coolant circuit confirmed that the coolant flow from the vane trailing edge slot has a significant impact on the heat transfer measured for the inner endwall. On the airfoil, the impact of the vane outer circuit is primarily limited to the gauges immediately downstream of the three rows of pressure-surface cooling holes supplied by this circuit, with the largest differences occurring at 5% span. This comparison illustrates that the vast majority of film cooling on the vane airfoil and most of the inner endwall comes from the vane inner circuit.

The data presented in this two-part paper shows that a complete heat transfer map is available for the film-cooled high-pressure vane of a stage and 1/2 turbine operating at design corrected conditions. Combined with heat-flux, temperature, and pressure data from the downstream rotor and purge cavity presented in earlier papers, this data presents a complete picture of the impact of inlet temperature profiles and cooling flow. These studies have shown that while many effects of cooling and profile shape can be explained by simple temperature reduction mixing models or by accounting for the inlet temperature, there are still important regions of the turbine that cannot be fully described by these principles. It is the complexity of these interactions that will keep researchers busy for many years to come.

6. ACKNOWLEDGEMENTS

Authors would like to thank the OSU GTL technical staff for performing this experimental work. This research was funded by the GE Aviation University Strategic Alliance Program. The technical assistance and guidance of Dr. Robert Bergholz of GEAE throughout this research is greatly appreciated.

7. REFERENCES

1. Goldstein, R.J., *Film Cooling*, in *Advances in Heat Transfer*, T.F. Irvine and J.P. Hartnett, Editors. 1971, Academic Press: New York. p. 321-379
2. Polanka, M.D., Ethridge, M.I., Cutbirth, J.M., and Bogard, D.M., 2000, "*Effects of Showerhead Injection on Film Cooling Effectiveness for a Downstream Row of Holes*". ASME 2000-GT-240.
3. Colban, W., Gratton, A., Thole, K.A., and Haendler, M., 2005, "*Heat Transfer and Film-Cooling Measurements on a Stator Vane with Fan-Shaped Cooling Holes*". ASME GT2005-58258.
4. Kost, F. and Mullaert, A., 2006, "*Migration of Film-Coolant from Slot and Hole Ejection at a Turbine Vane Endwall*". ASME GT2006-90355.
5. Bogard, D.G. and Thole, K.A., 2006, "*Gas Turbine Film Cooling*", *Journal of Propulsion and Power*, **22**(2): pp. 249-270.
6. Wagner, G., Ott, P., Vogel, G., and Naik, S., 2007, "*Leading Edge Film Cooling and the Influence of Shaped Holes at Design and Off-Design Conditions*". GT2007-27715, ASME Turbo Expo, Montreal, Canada.
7. Jonsson, M., Charbonnier, D., Ott, P., and von Wolfersdorf, J., 2008, "*Application of the Transient Heater Foil Technique for Heat Transfer and Film Cooling Effectiveness Measurements on a Turbine Vane Endwall*". GT2008-50451, ASME Turbo Expo, Berlin, Germany.
8. Charbonnier, D., Ott, P., Jonsson, M., Cottier, F., and Köbke, T., 2009, "*Experimental and Numerical Study of the Thermal Performance of a Film Cooled Turbine Platform*". GT2009-60306, ASME Turbo Expo, Orlando, FL.
9. Blair, M.F., 1974, "*An Experimental Study of Heat Transfer and Film Cooling on Large-Scale Turbine Endwalls*", *Journal of Heat Transfer*, **9**: pp. 524-529.
10. Langston, L.S., 1980, "*Crossflows in a Turbine Cascade Passage*", *Journal of Engineering for Power*, **102**: pp. 866-874.
11. Simon, T.W. and Piggush, J.D., 2006, "*Turbine Endwall Aerodynamics and Heat Transfer*", *Journal of Propulsion and Power*, **22**(2): pp. 301-312.
12. Friedrichs, S., Hodson, H.P., and Dawes, W.N., 1996, "*Distribution of Film-Cooling Effectiveness on a Turbine Endwall Measured Using the Ammonia and Diao Technique*", *Journal of Turbomachinery*, **118**(4): pp. 613-621, (Original Publication: ASME 95-GT-1).
13. Friedrichs, S., Hodson, H.P., and Dawes, W.N., 1997, "*Aerodynamic Aspects of Endwall Film-Cooling*", *Journal of Turbomachinery*, **119**(4): pp. 786-793, (Original Publication: 96-GT-208).
14. Friedrichs, S., Hodson, H.P., and Dawes, W.N., 1999, "*The Design of an Improved Endwall Film-Cooling*".

- Configuration*", **121**, (Original Publication: 98-GT-483).
15. Nicklas, M., 2001, "*Film-Cooled Turbine Endwall in a Transonic Flow Field: Part II--Heat Transfer and Film-Cooling Effectiveness*", *Journal of Turbomachinery*, **123**: pp. 720-729.
 16. Jenkins, S., Varadarajan, K., and Bogard, D.G., 2003, "*The Effects of High Mainstream Turbulence and Turbine Vane Film Cooling on the Dispersion of a Simulated Hot Streak*". ASME GT2003-38575.
 17. Varadarajan, K. and Bogard, D.G., 2004, "*Effects of Hot Streaks on Adiabatic Effectiveness for a Film Cooled Turbine Vane*". GT2004-54016.
 18. Barringer, M., Thole, K.A., Polanka, M.D., Clark, J.P., and Koch, P.J., 2009, "*Migration of Combustor Exit Profiles Through High Pressure Turbine Vanes*", *Journal of Turbomachinery*, **131**(2), (Original Publication: GT2007-27157).
 19. Barringer, M.D., Thole, K.A., and Polanka, M.D., 2009, "*An Experimental Study of combustor Exit Profile Shapes on Endwall Heat Transfer in High Pressure Turbine Vanes*", *Journal of Turbomachinery*, **131** (021009), (Original Publication: GT2007-27156).
 20. Kahveci, H.S., Haldeman, C.W., Mathison, R.M., and Dunn, M.G., 2011, "*Heat Transfer for the Film-Cooled Vane of a 1-1/2 Stage High-Pressure Transonic Turbine- Part I: Experimental Configuration and Data Review with Inlet Temperature Profile Effects*". GT2011-46570, TurboExpo 2011, Vancouver, Canada.
 21. Mathison, R.M., Haldeman, C.W., and Dunn, M.G., 2010, "*Heat Transfer for the Blade of a Cooled Stage and One-Half High-Pressure Turbine, Part I: Influence of Vane Cooling and Disk Cavity Purge Flow*". GT2010-22713, ASME Turbo Expo, Glasgow, Scotland.
 22. Mathison, R.M., Haldeman, C.W., and Dunn, M.G., 2010, "*Heat Transfer for the Blade of a Cooled One and One-Half Stage High-Pressure Turbine, Part II: Influence of Purge Cooling Variation*". GT2010-22715, ASME Turbo Expo, Glasgow, Scotland.
 23. Mathison, R.M., Haldeman, C.W., and Dunn, M.G., 2010, "*Aerodynamics and Heat Transfer for a Cooled One and One-Half Stage High-Pressure Turbine--Part I: Vane Inlet Temperature Profile Generation and Migration*". GT2010-22716, ASME Turbo Expo 2010, Glasgow, Scotland.
 24. Mathison, R.M., Haldeman, C.W., and Dunn, M.G., 2010, "*Aerodynamics and Heat Transfer for a Cooled One and One-Half Stage High-Pressure Turbine--Part II: Influence of Inlet Temperature Profile on Blade Heat Flux*". GT2010-22718, ASME Turbo Expo 2010, Glasgow, Scotland.
 25. Mathison, R.M., Haldeman, C.W., and Dunn, M.G., 2010, "*Aerodynamics and Heat Transfer for a Cooled One and One-Half Stage High-Pressure Turbine--Part III: Impact of Hot Streak Characteristics on Blade Row Heat Flux*". GT2010-23855, ASME Turbo Expo 2010, Glasgow, Scotland.
 26. Sen, B., Schmidt, D.L., and Bogard, D.G., 1996, "*Film Cooling with Compound Angle Holes: Heat Transfer*", *Journal of Turbomachinery*, **118**: pp. 800-806.
 27. Kahveci, H.S., "*The Influence of Film Cooling and Inlet Temperature Profile on Heat Transfer for the Vane Row of a 1-1/2 Stage Transonic High-Pressure Turbine*", Ph.D. Dissertation, Department of Mechanical Engineering, Ohio State University, 2010, pp. 286.